

Orientational structure and magnetic properties of a ferronematic in an external field

Yu. L. Raïkher, S. V. Burylov, and A. N. Zakhlevnykh

Institute of Mechanics of Continuous Media, Ural Scientific Center, Academy of Sciences of the USSR, Sverdlovsk, and A. M. Gorki State University, Perm

(Submitted 17 October 1985)

Zh. Eksp. Teor. Fiz. **91**, 542–551 (August 1986)

A study is made of the influence of an external magnetic field on the orientational structure of a ferronematic, representing a suspension of single-domain magnetic particles (“ferroparticles”) in a nematic liquid crystal. It is shown that a homogeneous orientation in a planar layer of a ferronematic is absolutely unstable on application of a magnetic field perpendicular to the direction of the initial orientation: the Fréedericksz transition has a zero threshold. The profiles of the distributions of the orientation and concentration of magnetic grains are obtained allowing for the segregation effects and the magnetization curves of a ferronematic are derived. It is shown that the initial susceptibility of a ferronematic layer is a quadratic function of the concentration of ferroparticles and that for systems encountered in experiments it may be several orders of magnitude higher than the magnetic susceptibility of a pure nematic.

1. INTRODUCTION

Ferronematics, i.e., highly disperse magnetic suspensions in which the carrier is a nematic liquid crystal, represent a new variety of liquid crystal materials of great interest from the general physics viewpoint, and also in respect of applications. Pinning of nematic molecules to the surfaces of magnetic grains in such systems makes it possible to create an extremely strong orientational coupling between ferroparticles and the liquid crystal matrix. Therefore, even at very low concentrations of the solid phase ($\sim 0.01\%$ by volume) the initial magnetic susceptibility of a liquid crystal suspension is between four and six orders of magnitude higher than the susceptibility of a pure nematic liquid crystal and a ferronematic is easily oriented by a relatively weak ($H \lesssim 10$ Oe) external field.¹

The problem of the orientational interaction of ferroparticles and a nematic matrix deserves a more detailed analysis. It is shown in Ref. 2, which gives the fundamentals of a theory of ferronematics, that suspensions of this type can exhibit two types of orientational behavior. In the first case when the concentration of particles is low (for an estimate see below) each particle oriented by an external field distorts the distribution of the director around it, irrespective of the other particles. Creation of such a distortion requires an energy $\sim Ka$, where K is the orientational elastic modulus and a is a typical size of a particle. In the interior of a sample of linear size R with a particle concentration c an increase in the elastic energy is of the order of $\Delta E_i \sim cKaR^3$. The texture of a sample represents a system of small ($\sim a$) isolated domains that disturb slightly the initial state of the liquid crystal matrix. However, the response of a suspension to a change in the orientation of the particles may be different: the distortion may be “smeared out” over the volume of the sample; local orientations of the director and the particle axes are then similar and they vary continuously from point

to point with a characteristic spatial scale R . In this state a change in the elastic energy is practically independent of the particle concentration (there are no distortions over distances $\sim a$) and it is governed by the product of the density of the Frank energy $\sim K/R^2$ and the volume of the sample, which gives $\Delta E_c \sim KR$. Comparing the increments ΔE_i and ΔE_c , we obtain the following expression for the critical concentration:

$$c_* \sim 1/aR^2, \quad (1)$$

above which we have $\Delta E_c < \Delta E_i$, so that rotations of the particles result in reorientation of the matrix. We thus find that it is in the range $c > c_*$ that the condition of a strong orientational coupling (collective behavior) is obeyed by the magnetic and liquid-crystal components of a ferronematic.

A familiar example of a ferronematic is a suspension of needle-shaped grains of the ferrite $\gamma\text{-Fe}_2\text{O}_3$ in the thermotropic nematic MBBA (Refs. 1 and 3). Above the temperature of the transition to the liquid-crystal phase, such suspensions are macroscopically isotropic and similar to ordinary magnetic liquids. Cooling induces a phase transition in the matrix and creates a long-range orientational order so that a ferronematic is formed. An estimate obtained using Eq. (1) shows that at the experimental^{1,3} concentrations $c \sim 10^{10}$ – 10^{11} cm⁻³ the collective behavior of a ferronematic is retained for samples with dimensions right down to $R_* \sim (ac)^{-1/2} \approx 15 \mu$; here, $a \approx 0.5 \mu$ is the length of a needle-shaped particle.

If cooling takes place in the absence of a magnetic field, a suspension is converted into a compensated ferronematic in which the macroscopic magnetization M vanishes. In such a sample the directions of the axes of all the particles are parallel to the director \mathbf{n} and the magnetic moments $\boldsymbol{\mu}$ are equally likely to assume the values $\mu\mathbf{n}$ and $-\mu\mathbf{n}$; we recall that the condition of strong coupling forbids the noncollin-

erarity of μ and \mathbf{n} . A ferronematic is created² by the application to a system of this kind of a single magnetic field pulse of amplitude $H > H_c$, where H_c is the coercive force of the magnetic particles (grains). Under the action of this pulse all the particles assume the same direction of the magnetic moments and a finite constant magnetization is established. An alternative method of magnetic ordering of a ferronematic is the application of a static field during the passage through the bleaching point.

In the early seventies, Brochard and de Gennes² formulated a continuum approach (see also the review in Ref. 4) to the description of a ferronematic based on generalization of the Frank potential of orientational elastic deformations in a liquid crystal. We shall use this theory to consider the Fréedericksz effect (see Ref. 5 for the case of pure nematic liquid crystals) in a ferronematic layer exhibiting collective behavior.

2. EQUILIBRIUM EQUATIONS FOR A PLANAR FERRONEMATIC LAYER

We shall consider an infinite planar ferronematic layer of thickness D with a planar texture and a strong coupling of the liquid-crystal molecules to the surfaces of the particles and to the layer boundaries. We shall select the origin of the coordinate system at the center of the layer, as shown in Fig. 1. We shall assume that the liquid phase of a ferronematic consists of needle-shaped single-domain magnetically hard ferrite grains magnetized along the principal axis. The magnetic moment of one such particle is $\mu = M_s v$, where v is the volume and M_s is the saturation magnetization of a ferrite. In the initial state the orientation of a sample is homogeneous, the particles are distributed uniformly over the volume of the layer, and the magnetic moments are parallel to the director \mathbf{n} and oriented in the same way, so that the magnetization of a ferronematic is $\mathbf{M} = M_s f \mathbf{n}$, where $f = cv$ is the volume concentration of the solid phase. The x axis in Fig. 1 will be regarded as the axis of the initial orientation. The magnetic field $\mathbf{H} = (0, H, 0)$ applied in the plane of the layer rotates the particles, as well as the director of the liquid-crystal molecules, creating an orientational deformation in the form of a torsional mode:

$$\mathbf{n} = [\cos \varphi(z), \sin \varphi(z), 0]; \quad (2)$$

the choice of the angle φ is explained in Fig. 1.

The volume density of the free energy of a ferronematic in an external field H can be written in the form

$$F = \frac{1}{2} \{ K_{11} (\text{div } \mathbf{n})^2 + K_{22} (\mathbf{n} \text{ curl } \mathbf{n})^2 + K_{33} [\mathbf{n} \text{ curl } \mathbf{n}]^2 \} - M_s f \mathbf{n} \mathbf{H} + (f k_B T / v) \ln f, \quad (3)$$

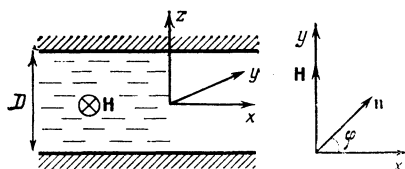


FIG. 1. Geometry of a ferronematic layer.

where K_{ii} are the orientational elastic moduli. The first three terms in Eq. (3) represent the usual Frank potential, and the remaining terms represent the energy of the interaction of the magnetic moments of the particles with the external field and the contribution associated with the mixing entropy. Following the treatment of Brochard and de Gennes² we ignored in Eq. (3) the diamagnetic effects because in the investigated range of fields ($H \approx 10$ Oe) they are extremely weak and we also disregarded the magnetic-dipole interaction of the particles because of their low concentration. The free energy $\mathcal{F} = \int F dV$ of a ferronematic with the orientational distribution given by Eq. (2) assumes the following form after the substitution of Eq. (3):

$$\mathcal{F} = \int dV \left[\frac{1}{2} K_{22} (\varphi')^2 - M_s f H \sin \varphi + \frac{k_B T}{v} f \ln f \right], \quad (4)$$

where the prime denotes differentiation with respect to z .

We can see from Eq. (4) that the functional \mathcal{F} depends on two functions: the angle of rotation of the director $\varphi(z)$ and the particle concentration $f(z)$. The equilibrium equations can be derived from Eq. (3) by independent variation of φ and f . The first condition ($\delta \mathcal{F} / \delta \varphi = 0$) gives

$$K_{22} \varphi''(z) + M_s f H \cos \varphi(z) = 0. \quad (5)$$

In the derivation of the second condition ($\delta \mathcal{F} / \delta f = 0$) we have to allow for the relationship $\int f dV = Nv$, corresponding to conservation of the total number N of the magnetic particles. Introducing the average density of the solid phase $\bar{f} = vN/V$, where V is the volume of the sample, we find that the equilibrium function $f(z)$ is given by

$$f = \bar{f} Q \exp[\rho \sin \varphi(z)], \quad Q = D \left\{ \int_{-D/2}^{D/2} \exp[\rho \sin \varphi(z)] dz \right\}^{-1}; \quad (6)$$

here, $\rho = M_s v H / k_B T$ is the Langevin parameter of the particles representing the ratio of their magnetic and thermal energies.

Equations (5) and (6) establish the relationship between the distribution of the particles and the orientation in a ferronematic. Since a strong coupling of the directions of the principal axes (and, consequently, of the magnetic moments of the particles) with the local director is assumed for a ferronematic, it is obvious that the particles accumulate in those parts of a sample where the directions of \mathbf{n} and \mathbf{H} are close ($\sin \varphi \ll 1$) migrating here from the regions with an unfavorable orientation. In our case the sources of the unfavorable orientation are the boundaries of the layer where an infinitely strong coupling of the liquid-crystal molecules to the wall of the layer is assumed: $\mathbf{n} \parallel \mathbf{x}$ at $z = \pm D/2$. A redistribution of the concentration of the magnetic impurity in an inhomogeneously oriented sample is predicted in Ref. 2 and is known as the segregation effect. An experimental observation of this effect in lyotropic ferronematics was reported in Ref. 6. It follows from Eq. (6) that segregation of magnetic particles becomes important if $\rho \gtrsim 1$. In the case of real ferronematics with the parameters taken from Refs. 1 and 3 this corresponds to the range of fields $H \gtrsim 0.1$ Oe, i.e., the homogeneity of the concentration must be allowed for even in the

range far from magnetic saturation of a ferronematic.

Substitution of Eq. (6) into Eq. (5) yields the integro-differential equation

$$\xi^2 \varphi'' + Q \exp(\rho \sin \varphi) \cos \varphi = 0, \quad \xi = (K_{22}/M_s \bar{f} H)^{1/2}, \quad (7)$$

where ξ is the magnetic coherence length representing the range of the orienting action of a wall in a ferronematic magnetized by a field H and characterized by a homogeneous distribution of the particles. In a planar layer the required solution $\varphi(z)$ should satisfy the boundary conditions

$$\varphi(\pm D/2) = 0, \quad \varphi'(0) = 0. \quad (8)$$

The first of these conditions corresponds to pinning of the nematic molecules by the boundaries of the layer, whereas the second represents symmetry of the orientational distribution in the ferronematic. Equation (7) has the first integral which, with the aid of the second condition in Eq. (8), can be represented in the form

$$1/2 \rho \xi^2 \varphi'^2 + Q [\exp(\rho \sin \varphi) - \exp(\rho \sin \varphi_m)] = 0. \quad (9)$$

Here, the constant φ_m represents the largest angle of deviation of the director from the initial orientation axis: $\varphi_m = \varphi(0)$. Solving Eq. (9) for dz , we obtain

$$dz = \mp \lambda Q^{-1/2} [\exp(\rho \sin \varphi_m) - \exp(\rho \sin \varphi)]^{-1/2} d\varphi; \quad (10)$$

Here, the symbols \mp refer to the upper and lower half-spaces $z \geq 0$, respectively (Fig. 1). A characteristic scale $\lambda = \xi \rho^{1/3}$ is independent of the field,

$$\lambda = (K_{22} v / 2 \bar{f} k_B T)^{1/2}, \quad (11)$$

and it is of the same order of magnitude as the thickness of a transition layer separating in an inhomogeneously oriented ferronematic the regions with the favorable and unfavorable mutual orientations of \mathbf{n} and \mathbf{H} . In the presence of segregation the parameter λ of a ferronematic plays the same role as the coherence length ξ in the case when $f = \text{const}$.

Integration of Eq. (10) in the range $z > 0$ subject to Eq. (7) gives

$$(D - 2z)/\lambda = 2Q^{-1/2} I(\varphi), \quad (12)$$

where

$$I(\varphi) = \int_0^\varphi [\exp(\rho \sin \varphi_m) - \exp(\rho \sin t)]^{-1/2} dt.$$

At $z = 0$ the angle of deviation of the director is maximal ($\varphi = \varphi_m$) and it follows from Eq. (12) that

$$D/\lambda = 2Q^{-1/2} I(\varphi_m). \quad (13)$$

Eliminating with the aid of Eq. (13) the integral coefficient Q in Eq. (12), we obtain an equation

$$1 - 2z/D = I(\varphi)/I(\varphi_m), \quad (14)$$

which defines in an implicit form the function $\varphi(z)$ representing the orientational profile of a ferronematic for a given value of φ_m . Using Eq. (10) to transform the integral in Eq. (6), we find that

$$Q = I(\varphi_m)/J(\varphi_m), \quad (15)$$

where

$$J(\varphi) = \int_0^\varphi \exp(\rho \sin t) [\exp(\rho \sin \varphi_m) - \exp(\rho \sin t)]^{-1/2} dt.$$

Substitution of Eq. (15) into Eq. (13) gives the equation

$$1/4 (D/\lambda)^2 = I(\varphi_m) J(\varphi_m), \quad (16)$$

which closes the system (14)–(16). The procedure used to solve the problem is as follows: first, we assume values of the field intensity, film thickness, and characteristics of a ferronematic and find φ_m from Eq. (16). Then, using this result, we find $\varphi(z)$ from Eq. (14) and finally use Eqs. (15) and (5) to plot the concentration distribution function $f(z)$.

3. ORIENTATIONAL PROFILE AND DISTRIBUTION OF THE PARTICLE CONCENTRATION IN A FERRONEMATIC

Simple considerations allow us to identify directly the difference between the manifestations of the Fréedericksz effect in a pure nematic and in a ferronematic. In the former case the effect in a planar [Eq. (8)] or a homeotropic texture has a threshold:

$$\varphi_m = \begin{cases} 0, & H < H_c, \\ \sim (H - H_c)^{1/2}, & H > H_c, \end{cases} \quad (17)$$

where H_c is a certain critical field (for details see Refs. 5 and 7), whereas in the case of a ferronematic the orientational homogeneity is disturbed even by an infinitesimally weak field (absolute instability). Such destabilization is clearly due to lowering of the symmetry of the free energy of Eq. (3), which now contains the dipole term $M_s \bar{f} \mathbf{n} \cdot \mathbf{H}$. Defining in accordance with the usual rules the total torque $\Gamma = -[\mathbf{n}, \delta \mathcal{F} / \delta \mathbf{n}]$ acting per unit volume of a ferronematic, we can readily show that $\Gamma = 0$ (equilibrium) is established only after distortion of the initial orientation.

Solving Eq. (16) for the case of weak fields satisfying the condition $\rho \varphi_m \ll 1$, we find that instead of the threshold behavior described by Eq. (17), in the case of a ferronematic the rotation of the director is continuous:

$$\varphi_m = \rho D^2 / 16 \lambda^2 = M_s \bar{f} H D^2 / 8 K_{22}, \quad (18)$$

i.e., the response of the orientation to an external magnetic field is linear and this response depends quadratically on the layer thickness. Therefore, the orientational ($\partial \varphi_m / \partial H$), and naturally the corresponding magnetic ($\partial M / \partial H$) initial susceptibilities of a ferronematic increase on increase in the layer thickness, since in the case of a thick layer the influence of the boundary conditions is less. In the same approximation ($\rho \varphi_m \ll 1$) the distribution of the orientation in a ferronematic is described by the parabolic profile

$$\varphi(z) = \varphi_m (1 - 4z^2/D^2) \quad (19)$$

with φ_m given by Eq. (18); the distribution of the concentration in the first order in respect of $\rho \varphi_m$ is

$$f(z) = \bar{f} [1 + \rho^2 D^2 (1 - 12z^2/D^2) / 48 \lambda^2].$$

As the field is increased, the rise of φ_m slows down

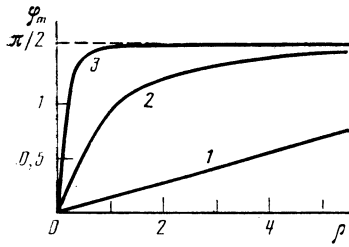


FIG. 2. Dependences of the angle of maximum rotation of the director on the dimensionless intensity of the magnetic field $\rho = M_s v H / k_B T$, plotted for layer thicknesses $D/\lambda = \sqrt{2}$ (curve 1), $2\sqrt{5}$ (curve 2), and 10 (curve 3).

compared with the linear law (18) and for $\rho \rightarrow \infty$ the function $\varphi_m(\rho)$ tends to a finite limit $\pi/2$. The asymptotic expansion corresponding to $\rho^{-1/2} \ll 1$ gives

$$\frac{\pi}{2} - \varphi_m = 2^{1/2} \rho^{-1/2} \begin{cases} \exp[-(D^2/2^{1/2} \pi \lambda^2) \rho^{1/2}], & D/\lambda < \pi/2, \\ \exp[-(D/2^{1/2} \lambda) \rho^{1/2}], & D/\lambda > \pi/2. \end{cases} \quad (20)$$

The expressions in Eq. (20) indicate a definite difference between the laws of approach to saturation of the orientation in thin ($2D/\pi\lambda < 1$) and thin ($2D/\pi\lambda > 1$) ferronematic layers. It will be clear from a later discussion that this difference is a consequence of the fact that in a thin sample the formation of a natural boundary concentration layer of width $\sim \pi\lambda/4$ is not possible. Figure 2 gives the results of a numerical calculation and it illustrates the behavior of the function $\varphi_m(\rho)$ for arbitrary values of the argument. We can see that the thicker the layer, the easier it is to induce a change in the orientation in a central part of the layer by the application of a magnetic field.

Moreover, the concentration profiles of a ferronematic are different for different thicknesses of a layer. The quantity Q [see Eq. (6)] representing the relative concentration of particles near a wall [$Q = f(\pm D/2)/\bar{f}$] is described by the following expressions in the limit $\rho^{-1/2} \ll 1$:

$$Q \exp \rho = \begin{cases} (\pi\lambda/D)^2, & 2D/\lambda\pi < 1, \\ 1, & 2D/\lambda\pi > 1. \end{cases} \quad (21)$$

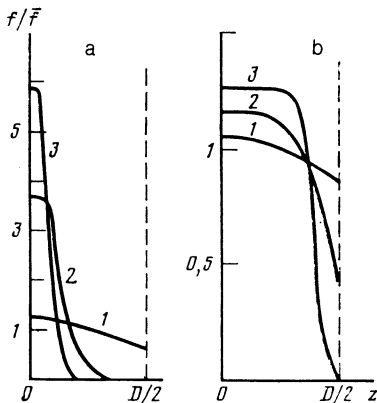


FIG. 3. Distribution of the composition in ferronematic layers of different thickness: a) $D/\lambda = \sqrt{2}$ for $\rho = 2.2$ (curve 1), 10 (curve 2), and 50 (curve 3); b) $D/\lambda = 10$ for $\rho = 0.24$ (curve 1), 1.1 (curve 2), and 5.3 (curve 3).

If $(2D/\lambda\pi) > 1$, this result is identical with the asymptotic expression for a layer of infinite width (half-space) derived in Ref. 2. Figure 3 shows the total concentration distributions $f(z)$ deduced numerically from Eqs. (6), (15), and (16). In the case of thick samples (Fig. 3b) subjected to a strong field the results demonstrate clearly the formation of a planar $f = \text{const}$ profile separated from the walls by narrow transition zones of width $\delta \approx \pi\lambda/4$. If $D/\delta \gg 1$, this case differs little from that of a layer of infinite thickness.

In the case of thin samples the transition zone occupies almost the whole of the layer volume (Fig. 3a). We can estimate the thickness of this zone by modifying the method used in Ref. 2 to determine δ in the limit $D/\lambda \rightarrow \infty$. We shall write down the equation of state for an ideal gas of magnetic particles in a ferronematic in the form

$$pz = N_0 k_B T,$$

where p is the osmotic pressure and $N_0 = \bar{f}D/2v$ is the number of particles in a ferronematic per unit area of its boundary. In a strong field when the principal axes of the particles tend to become aligned along the direction of \mathbf{H} , these particles leave the wall region so that an "empty" zone of thickness δ forms near the boundary. The following work is done on the isothermal compression of the "gas":

$$\Delta A = - \int_{D/2}^{D/2-\delta} p dz = \frac{\bar{f} D k_B T}{2v} \ln \frac{D}{D-2\delta},$$

and a finite elastic distortion energy $\Delta E \approx (K_{22}/\delta^2)\delta = K_{22}/\delta$ appears. Minimization of the sum $\Delta A + \Delta E$ with respect to δ gives

$$\delta^2 + (4\lambda^2/D)\delta - 2\lambda^2 = 0, \quad (22)$$

where λ is defined by Eq. (11). Solving Eq. (22), we find that if $\rho \gg 1$, then the equilibrium thickness of the transition zone is

$$\delta = \begin{cases} 1/2 D [1 - (D/2^{1/2} \lambda)^2], & D/2^{1/2} \lambda < 1, \\ \lambda [2^{1/2} - 2\lambda/D], & D/2^{1/2} \lambda > 1. \end{cases} \quad (23)$$

In the limit $D/\lambda \rightarrow \infty$ Eq. (23) gives the result obtained in Ref. 2 for half-space: $\delta \approx 2^{1/2} \lambda$. In the case of thin layers ($D/2^{1/2} \lambda < 1$) the compression of the concentration profile is prevented by the entropy elasticity of a gas of particles, which ensures a finite (although small) width of the distribution $f(z)$.

It therefore follows from Fig. 3 and Eq. (23) that a compression of a ferronematic layer occurs in strong fields: the thickness of the layer decreases (and the concentration of the particles in the central region becomes higher) and this layer becomes separated from the solid boundaries by transition zones where the nematic is practically impurity-free. The effective transverse size of a ferronematic layer is $D - 2^{3/2} \lambda$ in the case of thick samples and $D^3/8\lambda^2$ in the case of thin samples. In other words, the segregation effect results in a field-induced stratification of a ferronematic.

The orientational profiles of ferronematic samples of different thickness are plotted in Fig. 4. Curve 1 in both parts of this figure is described well by Eq. (19). Allowing for the

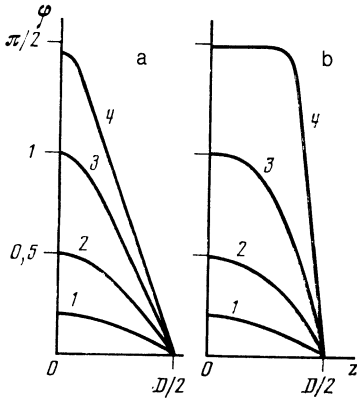


FIG. 4. Profiles of the orientation in ferronematic layers of different thickness: a) $D/\lambda = \sqrt{2}$ for $\rho = 1.5$ (curve 1), 3.5 (curve 2), 8.3 (curve 3), and 50 (curve 4); b) $D/\lambda = 10$ for $\rho = 0.016$ (curve 1), 0.087 (curve 2), 0.24 (curve 3), and 5.3 (curve 4).

condition of a strong coupling of the director to the orientations of the particle axes, we can readily understand the nature of the texture which appears in a strong field. In this case the distribution of the concentration in a sample can be regarded approximately as step-like:

$$f = \begin{cases} \text{const}, & 0 < |z| < D/2 - \delta, \\ 0, & D/2 - \delta < |z| < D/2. \end{cases}$$

The boundary of the magnetic part of the layer where all the particles are oriented along the field now acts as a new wall where the director ($\mathbf{n} \parallel y$) is pinned at right-angles to the director on the solid wall ($\mathbf{n} \parallel x$). The layer confined by these boundaries is filled with a pure nematic; the orientational state of this nematic is governed by the boundary conditions and represents a torsional structure with a helical pitch of 4δ . The distribution of the director $\varphi(z)$ is linear along the z axis: see curves denoted by 4 in Figs. 4a and 4b.

4. MAGNETIZATION OF A FERRONEMATIC

In the case of a strong coupling between magnetic particles and the liquid crystal matrix (collective behavior) the magnetization of an element of volume of a ferronematic is parallel to the local director, i.e., $\mathbf{M} = M_s \mathbf{f}$. In the orientation described by Eq. (2), the vector \mathbf{M} has the components

$$\mathbf{M} = [M \cos \varphi(z), M \sin \varphi(z), 0], \quad (24)$$

where $M = M_s f(z)$ is the local saturation magnetization of the ferronematic. Therefore, the distribution of the magnetization is governed by the combination of the profiles describing the orientation and composition. In the absence of a field the vector \mathbf{M} is directed along the initial orientation axis: $M_x = M_0$, $M_y = 0$, and in this case throughout a sample we have the constant magnetization $M_0 = M_s \bar{f}$. In weak fields ($\rho \ll 4\lambda/D$), we find that Eqs. (18) and (19) give

$$\frac{M_x}{M_0} = 1 - \frac{1}{2} \left[\frac{M_0 H}{8K_{22}} (D^2 - 4z^2) \right]^2, \quad \frac{M_y}{M_0} = \frac{M_0 H}{8K_{22}} (D^2 - 4z^2). \quad (25)$$

The formulas in Eq. (25) show that such a ferronematic

exhibits a linear response of the magnetization in the direction of an external field. It follows from Eq. (25) that the initial susceptibility $\chi = \partial M_y / \partial H$ depends on the coordinates and vanishes at the boundaries of the layer, where the director is rigidly locked. Averaging over the transverse cross section gives

$$\bar{\chi} = \frac{2}{D} \int_0^{D/2} \chi dz = \frac{M_0^2 D^2}{12K_{22}}. \quad (26)$$

Using the parameters of a ferronematic taken from Refs. 1 and 3, we estimate that the susceptibility is $\bar{\chi} \approx 4 \cdot 10^{-2}$ if $M_0 \approx 4 \times 10^{-2} G$ and $D \sim 10^{-2} \text{ cm}$. This susceptibility is five orders of magnitude greater than the value reported in Ref. 5 for pure MBBA ($\chi = 1.23 \cdot 10^{-7}$) at 19°C . This comparison demonstrates the enormous enhancement of the magnetic properties of a nematic by the addition of just a small amount (0.01% by volume) of the magnetic phase.

A general idea of the distribution of $M(z)$ in strong fields can be obtained from Figs. 3 and 4, which demonstrate that as the field in a ferronematic layer is increased, a magnetic core is formed where the directions of \mathbf{M} and \mathbf{H} are close to one another. However, it is more interesting to consider the magnetization components averaged over the cross section of a layer and this can be done using Eqs. (6), (15), and (24), which give

$$\begin{aligned} \frac{\bar{M}_x}{M_0} &= \frac{2}{\rho J(\varphi_m)} [\exp(\rho \sin \varphi_m) - 1]^{1/2}, \\ \frac{\bar{M}_y}{M_0} &= \frac{1}{J(\varphi_m)} \int_0^{\varphi_m} \exp(\rho \sin t) \\ &\quad \times [\exp(\rho \sin \varphi_m) - \exp(\rho \sin t)]^{-1/2} \sin t dt. \end{aligned} \quad (27)$$

Asymptotic dependences obtained by averaging the formulas in Eq. (25) in the case when $\rho \varphi_m \ll 1$ and those obtained using Eqs. (20) and (21) when $\rho^{-1/2} \ll 1$ yield the following expressions in weak fields

$$\bar{M}_x/M_0 = 1 - 1/60 \rho^2 (D/\lambda)^4, \quad \bar{M}_y/M_0 = 1/24 \rho (D/\lambda)^2,$$

whereas in strong fields the expression depends on the thickness:

$$\text{a) thin layers } (2D/\pi\lambda \ll 1)$$

$$\bar{M}_x/M_0 = 4\pi\lambda^2/D^2\rho, \quad \bar{M}_y/M_0 = 1 - 2^{1/2}\pi\lambda^2/D^2\rho^{3/2};$$

$$\text{b) thick layers } (2D/\pi\lambda \gg 1)$$

$$\bar{M}_x/M_0 = 4\lambda/D\rho, \quad \bar{M}_y/M_0 = 1 - 2^{1/2}\lambda/D\rho^{3/2}.$$

The magnetization curves of Eq. (27), plotted using the results of numerical calculations of the functions $\varphi(z)$ and $f(z)$, are shown in Fig. 5 for the directions parallel and perpendicular to the external field. We can see that the rate of magnetization of a ferronematic along the applied field (y axis) increase on increase in the thickness of the layer: saturation occurs at lower values of ρ . This can easily be understood bearing in mind that the particles concentrated in the

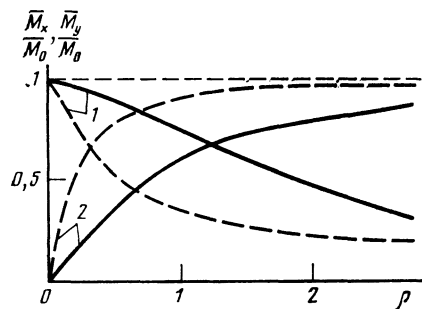


FIG. 5. Variation of the magnetization in a ferronematic layer of thickness $D/\lambda = 2\sqrt{5}$ (continuous curves) and $D/\lambda = 10$ (dashed curves). 1) Components \bar{M}_x ; 2) Components \bar{M}_y .

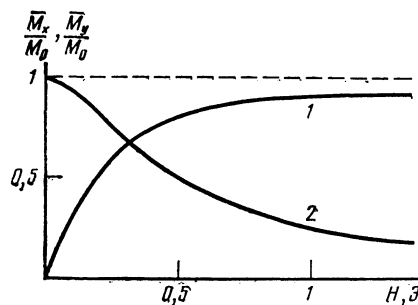


FIG. 7. Variation of the magnetization in a ferronematic layer of thickness $D = 200 \mu$: 1) parallel to the applied field (\bar{M}_y/\bar{M}_0); 2) along the initial orientation (\bar{M}_x/\bar{M}_0).

central region are rotated more readily in an external field the weaker the influence of the orienting influence of the walls.

Although only fragmentary data are at present available on the magnetic properties of ferronematics, one would hope that a comparison with the experimental results would be possible later so that it is useful to report the results of a calculation of the composition profiles and of the magnetization curves of a ferronematic, the parameters of which correspond to those of suspensions of needle-like single-domain $\gamma\text{-Fe}_2\text{O}_3$ particles in MBBA, reported in Refs. 1 and 3. For these systems we have $K_{22} = 3.4 \times 10^{-7}$ dyn, $v \approx 5 \times 10^{-16}$ cm³, and $\bar{f} \sim 10^{-5}$, so that the characteristic length of Eq. (11) is estimated to be

$$\lambda = (K_{22}v/2\bar{f}k_B T)^{1/2} \approx 150 \mu$$

at room temperature. Assuming a layer thickness $D = 200 \mu$ typical of experiments, we reached the conclusion that the inequality $D/2^{1/2}\lambda \lesssim 1$ is obeyed and it then follows from Eq. (23) that in a sufficiently strong external field a layer struc-

ture should form and it should consist of a thin central layer of a ferronematic with nematical liquid crystals on both sides, i.e., the sample should become strongly stratified. Figure 6 shows the results of a numerical calculation confirming the above qualitative considerations. The dependences $M(H)$ shown in Fig. 7 demonstrate that the magnetic (and, consequently, the orientational) saturation of a ferronematic layer occurs in fields of ~ 1 Oe, i.e., two or three orders of magnitude less than those required in the case of a pure nematic.

The analysis given in Secs. 2–4 corresponds to just one of the three classical geometries^{5,7} in which the Fréedericksz effect is observed. However, all the significant features of this effect in a ferronematic are in fact manifested equally in the other two configurations. The textures in question differ from that investigated above only in respect of the orientational deformation (transverse and longitudinal bending modes instead of a torsional mode), which is easily allowed for by redefinition of the orientational elastic constant.

The authors are grateful to M. I. Shliomis for his interest and to participants of a Moscow seminar on liquid crystals for valuable discussions.

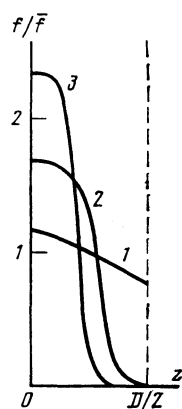


FIG. 6. Distribution of the composition in a ferronematic layer of thickness $D = 200 \mu$ in fields $H = 0.16$ Oe (curve 1), 1.3 Oe (curve 2), and 5.3 Oe (curve 3).

- ¹J. Rault, P. E. Cladis, and J. P. Burger, *Phys. Lett. A* **32**, 199 (1970).
- ²F. Brochard and P. G. de Gennes, *J. Phys. (Paris)* **31**, 691 (1970).
- ³S.-H. Chen and N. M. Amer, *Phys. Rev. Lett.* **51**, 2298 (1983).
- ⁴E. I. Kats, V kn.: *Fizicheskie metody izucheniya molekul i nadmolekulyarnykh struktur. Materialy shkoly LIYaF* (in: *Physical Methods for Investigation of Molecules and Supramolecular Structures: Proc. School at Leningrad Institute of Nuclear Physics*), Leningrad, 1979, p. 107.
- ⁵P. G. de Gennes, *The Physics of Liquid Crystals*, Clarendon Press, Oxford, 1974 (Russ. transl., Mir, M., 1977), Chap. 3.
- ⁶L. Liebert and A. M. Figueiredo Neto, *J. Phys. Lett.* **45**, L173 (1984).
- ⁷M. J. Stephen and J. P. Straley, *Rev. Mod. Phys.* **46**, 617 (1974).

Translated by A. Tybulewicz